ISSN: 2224-5286 (Print)
ISSN: 2518-1491 (Online)

ACADEMIC SCIENTIFIC JOURNAL OF CHEMISTRY

№2
2026

ISSN 2518-1491 (Online),
ISSN 2224-5286 (Print)

CENTRAL ASIAN ACADEMIC
RESEARCH CENTER

ACADEMIC SCIENTIFIC JOURNAL OF CHEMISTRY

2 (467)

APRIL – JUNE 2026

PUBLISHED SINCE JANUARY 1947
PUBLISHED 4 TIMES A YEAR

ALMATY

ACADEMIC SCIENTIFIC JOURNAL OF CHEMISTRY
ISSN 2518-1491 (Online),
ISSN 2224-5286 (Print)

Owner: «Central Asian Academic Research Center» LLP (Almaty).

The certificate of registration of a periodical printed publication in the Committee of information of the Ministry of Information and Social Development of the Republic of Kazakhstan **№ KZ23VPY00121156,**
issued 05.06.2025

Thematic scope: *organic chemistry, inorganic chemistry, catalysis, electrochemistry and corrosion, pharmaceutical chemistry and technology.*

Periodicity: 4 times a year.

http://chemistry-technology.kz/index.php/en/arhiv

«ACADEMIC SCIENTIFIC JOURNAL OF CHEMISTRY».
ISSN 2518-1491 (Online),
ISSN 2224-5286 (Print)
Собственник: Республиканское общественное объединение ТОО «Центрально-азиатский академический научный центр» (г. Алматы).
Свидетельство о постановке на учет периодического печатного издания в Комитете информации Министерства информации и общественного развития Республики Казахстан **№ KZ23VPY00121156,** выданное 05.06.2025 г.
Тематическая направленность: *органическая химия, неорганическая химия, катализ, электрохимия и коррозия, фармацевтическая химия и технологии.*
Периодичность: 4 раз в год.
http://chemistry-technology.kz/index.php/en/arhiv

«ACADEMIC SCIENTIFIC JOURNAL OF CHEMISTRY»
ISSN 2518-1491 (Online),
ISSN 2224-5286 (Print)
Меншіктенуші: «Орталық Азия академиялық ғылыми орталығы» ЖШС (Алматы қ.).
Қазақстан Республикасының Ақпарат және қоғамдық даму министрлігінің Ақпарат комитетінде 05.06.2025 ж. берілген **№ KZ23VPY00121156** мерзімдік басылым тіркеуіне қойылу туралы куәлік.
Тақырыптық бағыты: *органикалық химия, бейорганикалық химия, катализ, электрохимия және коррозия, фармацевтикалық химия және технологиялар.*
Мерзімділігі: жылына 4 рет.
http://chemistry-technology.kz/index.php/en/arhiv

CONTENTS

МАЗМҰНЫ

СОДЕРЖАНИЕ

ACADEMIC SCIENTIFIC JOURNAL OF CHEMISTRY
ISSN 2224–5286
Volume 2.
Number 467 (2026), 55–74

https://doi.org/10.32014/2026.2518-1491.363

IRSTI 31.17.15
UDC 549.753.1: 543.573

© Baikenov Ye.A., Safarov R.Z.*, Shomanova Zh.K.*, 2026.
L.N. Gumilyov Eurasian National University, Astana, Kazakhstan.
E-mail: safarov_rz@enu.kz

TGA-DSC QUANTIFICATION OF CALCITE WITH XRF CROSS-VALIDATION IN CENTRAL KAZAKHSTAN MANGANESE ORES

Baikenov Yerlan — PhD student, L.N. Gumilyov Eurasian National University, Astana, Kazakhstan, E-mail: baikenov_yea_1@enu.kz, https://orcid.org/0009-0003-4582-111X;
Safarov Ruslan — candidate of chemical sciences, L.N. Gumilyov Eurasian National University, Astana, Kazakhstan; Kh. Dosmukhamedov Atyrau University, Atyrau, Kazakhstan, E-mail: safarov_rz@enu.kz, https://orcid.org/0000-0003-2158-6330;
Shomanova Zhanat — Doctor of technical sciences, Margulan University, Pavlodar, Kazakhstan, E-mail: zshoman@yandex.ru, https://orcid.org/0000-0002-3290-0113.

Abstract. Thermogravimetric analysis (TGA) is used to estimate calcite content in ore feedstock through the mass loss in the $CaCO_3$ decarbonation window (700–850 °C). In manganese ores this interval overlaps with the $MnO_2 \rightarrow Mn_2O_3 \rightarrow Mn_3O_4$ reduction chain and silicate dehydroxylation, making unambiguous attribution of the mass loss to carbonate decomposition impossible. X-ray fluorescence (XRF) provides only the bulk Ca content without phase assignment. A cross-validation protocol is proposed to test the carbonate hypothesis. Since $CaCO_3 \rightarrow CaO + CO_2$ releases 43.97 wt.% CO_2, the calcite fraction from TGA equals the mass loss divided by 0.4397; an independent XRF estimate uses the molar ratio $M(CaCO_3)/M(Ca) = 2.4973$. Agreement within a relative discrepancy of about 5 % ($|\delta| \lesssim 5$ %, the propagated 1σ limit) indicates that the mass loss is attributable to decarbonation. The protocol is tested on two contrasting ores from Central Kazakhstan: carbonate-bearing Bogach (positive control) and silicate-bearing Zhaksy (negative control). For Bogach the two estimates agree (14.33 wt.% TGA, 13.58 wt.% XRF; $\delta = +5.2$ %), confirming a carbonate origin of the high-temperature mass loss. These mutually consistent bulk values nonetheless exceed the phase-resolved XRD value (8.4 wt.%), so the protocol screens for carbonate-bound Ca rather than quantifying calcite absolutely. For Zhaksy $\delta = +70.5$ %, clearly violating the hypothesis; two independent checks corroborate this: the DSC heat effect (537 J g^{-1}) is sixteen times higher than expected for the XRF-based calcite content, and the dTG–DSC minimum offset of +77 °C (versus +9 °C for Bogach) indicates different underlying processes.

The protocol flags samples for which naive TGA-based estimation would overestimate calcite and directs them to phase-resolved analysis (XRD Rietveld, TG–MS).

Keywords: manganese ore, calcite quantification, thermogravimetric analysis, differential scanning calorimetry, X-ray fluorescence, Bogach deposit

Financing. *The given research was carried out within the framework of a project funded by the Science Committee of the Ministry of Science and Higher Education of the Republic of Kazakhstan (Grant No. AP23488858).*

For citations: Baikenov Ye.A., Safarov R.Z., Shomanova Zh.K. TGA-DSC quantification of calcite with XRF cross-validation in Central Kazakhstan manganese ores. Academic Scientific Journal of Chemistry, 2026. — No.2. – P. 55–74. DOI: https://doi.org/10.32014/2026.2518-1491.363

Л.Н. Гумилев атындағы Еуразия ұлттық университеті, Астана, Қазақстан.
E-mail: safarov_rz@enu.kz

ОРТАЛЫҚ ҚАЗАҚСТАН МАРГАНЕЦ КЕНДЕРІНДЕГІ КАЛЬЦИТТІ ТГА-ДСК ӘДІСІМЕН САНДЫҚ БАҒАЛАУ ЖӘНЕ РФА БОЙЫНША КРОСС-ВАЛИДАЦИЯ

Байкенов Ерлан — докторант, Л.Н. Гумилев атындағы Еуразия ұлттық университеті, Астана, Қазақстан,
E-mail: baikenov_yea_1@enu.kz, https://orcid.org/0009-0003-4582-111X;
Сафаров Руслан — химия ғылымдарының кандидаты, Л.Н. Гумилев атындағы Еуразия ұлттық университеті, Астана, Қазақстан; Х. Досмұхамедов атындағы Атырау университеті, Атырау, Қазақстан,
E-mail: safarov_rz@enu.kz, https://orcid.org/0000-0003-2158-6330;
Шоманова Жанат — техникалық ғылымдарының докторы, Әлкей Марғұлан атындағы Павлодар педагогикалық университеті, Павлодар, Қазақстан,
E-mail: zshoman@yandex.ru, https://orcid.org/0000-0002-3290-0113.

Аннотация. Термогравиметриялық талдау (ТГА) кальцит мөлшерін $CaCO_3$ декарбонизация интервалындағы (700–850 °C) масса жоғалуы арқылы бағалауға қолданылады. Марганец кендерінде бұл интервал $MnO_2 \rightarrow Mn_2O_3 \rightarrow Mn_3O_4$ тотықсыздану тізбегімен және силикаттардың дегидроксилденуімен қабаттасады, бұл масса жоғалуын карбонатты реакцияға бір мәнді жатқызуды мүмкін емес етеді. Рентгенфлуоресценттік талдау (РФА) Ca-ның тек жалпы мөлшерін фазалық байланыссыз береді. Карбонатты гипотезаны айқастырып тексеру хаттамасы ұсынылды. $CaCO_3 \rightarrow CaO + CO_2$ ыдырауы кезінде 43,97 мас.% CO_2 бөлінетіндіктен, ТГА бойынша кальцит мөлшері масса жоғалуын 0,4397-ге бөлуге тең; РФА бойынша тәуелсіз бағалау $M(CaCO_3)/M(Ca) = 2,4973$ мольдік қатынасын пайдаланады. Шамамен 5% шегіндегі ($|\delta| \lesssim 5$ %, есептелген 1σ-шегі) сәйкестік масса жоғалуының декарбонизациядан туындайтынын көрсетеді. Хаттама

Орталық Қазақстанның екі қарама-қарсы кенінде сыналды: карбонатты Боғаш (оң бақылау) және силикатты Жақсы (теріс бақылау). Боғаш үшін екі бағалау үйлеседі (14,33 мас.% ТГА, 13,58 мас.% РФА; δ = +5,2 %), бұл жоғары температуралы масса жоғалуының карбонатты шығу тегін растайды. Дегенмен бұл өзара үйлесімді жалпы мәндер фазалық сезімтал XRD бағалауынан (8,4 мас.%) асып түседі, сондықтан хаттама кальцитті абсолютті анықтау емес, карбонатты-байланысқан Ca үшін үйлесімділікті тексеру құралы болып табылады. Жақсы үшін δ = +70,5 %, гипотеза бұзылады; екі тәуелсіз критерий мұны растайды: ДСК жылу эффектісі (537 Дж·г$^{-1}$) РФА бойынша кальцитке күтілгеннен он алты есе жоғары, ал dТГ–ДСК минимумдарының +77 °C ығысуы (+9 °C Боғашқа қарсы) процестердің әртүрлі табиғатын көрсетеді. Хаттама тікелей ТГА қолдану кальцитті асыра бағалайтын үлгілерді анықтап, оларды фазалық сезімтал талдауға (XRD–Ритвельд, ТГ–МС) жібереді.

Түйін сөздер: марганец кені, кальцит мөлшерін бағалау, термогравиметриялық талдау, дифференциалды сканерлеуші калориметрия, рентгенфлуоресценттік талдау, Боғаш кен орны

© Байкенов Е.А.[1], Сафаров Р.З.[1,2]*, Шоманова Ж.К.[3]*, 2026.
[1]Евразийский национальный университет им. Л.Н. Гумилёва, Астана, Казахстан.
[2]Атырауский университет имени Х. Досмухамедова, Атырау, Казахстан;
[3] Павлодарский педагогический университет имени Алкей Маргулан, Павлодар, Казахстан.
E-mail: safarov_rz@enu.kz

КОЛИЧЕСТВЕННАЯ ОЦЕНКА КАЛЬЦИТА МЕТОДОМ ТГА-ДСК С КРОСС-ВАЛИДАЦИЕЙ ПО РФА В МАРГАНЦЕВЫХ РУДАХ ЦЕНТРАЛЬНОГО КАЗАХСТАНА

Байкенов Ерлан — докторант, Евразийский национальный университет имени Л.Н. Гумилёва, Астана, Казахстан,
E-mail: baikenov_yea_1@enu.kz, https://orcid.org/0009-0003-4582-111X;
Сафаров Руслан — кандидат химических наук, Евразийский национальный университет имени Л.Н. Гумилёва, Астана, Казахстан; Атырауский университет имени Х. Досмухамедова, Атырау, Казахстан,
E-mail: safarov_rz@enu.kz, https://orcid.org/0000-0003-2158-6330;
Шоманова Жанат — доктор технических наук, Павлодарский педагогический университет имени Алкей Маргулан, Павлодар, Казахстан,
E-mail: zshoman@yandex.ru, https://orcid.org/0000-0002-3290-0113.

Аннотация: Термогравиметрический анализ (ТГА) применяется для оценки содержания кальцита через масс-потерю в интервале декарбонизации $CaCO_3$ (700–850 °C). В марганцевых рудах этот интервал перекрывается с восстановительными превращениями $MnO_2 \rightarrow Mn_2O_3 \rightarrow Mn_3O_4$ и дегидроксилированием силикатов, что делает однозначное отнесение масс-потери к карбонатной реакции невозможным. Рентгенофлуоресцентный анализ (РФА) даёт лишь валовое содержание Ca без

фазовой привязки. Предложен протокол перекрёстной проверки карбонатной гипотезы. Поскольку при разложении $CaCO_3 \rightarrow CaO + CO_2$ выделяется 43,97 мас.% CO_2, содержание кальцита по ТГА равно масс-потере, делённой на 0,4397; независимая оценка по РФА использует молярное отношение $M(CaCO_3)/M(Ca) = 2{,}4973$. Согласие в пределах относительного расхождения около 5 % ($|\delta| \lesssim 5$ %, рассчитанный 1σ-предел) указывает на карбонатное происхождение масс-потери. Протокол испытан на двух контрастных рудах Центрального Казахстана: карбонатной руде Богач (положительный контроль) и силикатной руде Жаксы (отрицательный контроль). Для Богач обе оценки согласуются (14,33 мас. % ТГА, 13,58 мас. % РФА; $\delta = +5{,}2$ %), что подтверждает карбонатное происхождение высокотемпературной масс-потери. Эти взаимно согласованные валовые значения, тем не менее, превышают фазочувствительную оценку XRD (8,4 мас.%), поэтому протокол служит инструментом проверки согласованности для карбонатно-связанного Ca, а не абсолютного определения кальцита. Для Жаксы $\delta = +70{,}5$ %, гипотеза нарушена; два независимых критерия подтверждают это: тепловой эффект ДСК (537 Дж·г$^{-1}$) в шестнадцать раз превышает ожидаемый для содержания кальцита по РФА, а смещение минимумов dТГ–ДСК +77 °C (против +9 °C для Богач) указывает на разную природу процессов. Протокол выявляет пробы, для которых прямое применение ТГА завышает содержание кальцита, и направляет их на фазочувствительный анализ (XRD–Ритвельд, ТГ–МС).

Ключевые слова: марганцевая руда; количественная оценка кальцита; термогравиметрический анализ; дифференциальная сканирующая калориметрия; рентгенофлуоресцентный анализ; месторождение Богач

Introduction. Manganese ores of the Atasu mineralogical province in Central Kazakhstan supply feedstock for the domestic ferroalloy industry (Gordon et al., 2018; Matsanga et al., 2025) and are considered as a raw material for trimanganese tetraoxide (Mn_3O_4) pigment production (Safarov et al., 2021). The province is dominated by hydrothermal–sedimentary deposits of the Atasu type (Brusnitsyn et al., 2021), which carry oxide–carbonate parageneses with cryptomelane, hollandite, braunite, hausmannite and a variable carbonate fraction. The Bogach deposit (Karaganda region) and the Zhaksy deposit (Akmola region) are end-member representatives of this paragenesis. Bogach is an oxide–carbonate ore enriched in calcite, whereas Zhaksy is a silicate-bearing braunite ore with a negligible carbonate component (Safarov et al., 2021, 2025). Quantification of the Ca-bearing phase in such ores is a prerequisite for predicting their pyrometallurgical behaviour and for selecting the appropriate beneficiation route (Matsanga et al., 2025).

Calcite acts simultaneously as a gangue mineral and as a carbonate precursor during high-temperature processing of Mn ore. Its decarbonation releases CaO that participates in slag formation and conditions the charge during calcination and sintering stages (Gordon et al., 2018). At the same time, calcite imposes a substantial energy penalty on the smelting stage. The decarbonation reaction $CaCO_3 \rightarrow CaO + CO_2$ is endothermic with a standard enthalpy of about 178 kJ mol^{-1} (Rodriguez-Navarro et al.,

2009). Quantification of the calcite mass fraction therefore enters the energy balance of the smelting stage and the estimate of CO_2 released during pre-sintering of Mn ore feedstock (Gordon et al., 2018). For deposits with variable Ca content along the body, such as Bogach and Zhaksy, this requirement translates into a need for an applicable analytical protocol that can be deployed on many bulk samples without resorting to slow phase-resolved methods.

Reliable calcite quantification in this matrix calls for an analytical decision rule that flags samples in which the decarbonation interpretation of the TGA signal becomes unreliable. The present work develops such a rule by combining two routinely available bulk methods – TGA and XRF – and using the discrepancy between the two derived calcite estimates as a diagnostic of carbonate-bound Ca. The protocol is applied to two contrasting ores from Central Kazakhstan: the carbonate-bearing Bogach ore as a positive control and the silicate-bearing Zhaksy ore as a negative control. The objectives are (i) to derive the consistency criterion from propagated measurement uncertainties rather than postulating it, (ii) to apply the criterion to a paired comparison and interpret the resulting discrepancy values in terms of Ca-phase speciation, and (iii) to support the interpretation by an independent dTG–DSC co-registration test and by a plausibility check based on the standard enthalpy of $CaCO_3$ decarbonation.

Literary review.

Quantification of calcite in a manganese matrix is non-trivial because the decarbonation window of pure calcite at 10 K min^{-1} under flowing N_2 lies between 700 and 850 °C (Zhuang et al., 2025), a range consistent with data obtained in flowing air at 2–15 K min^{-1} (Rodriguez-Navarro et al., 2009). The decarbonation window overlaps with two competing thermal processes specific to Mn-rich ores. The reduction chain $MnO_2 \rightarrow Mn_2O_3 \rightarrow Mn_3O_4$ proceeds through 400–1000 °C with mass losses of up to several wt.% (Song et al., 2023), and slow oxygen release from Mn(III)-bearing oxide phases extends the upper edge of this interval (Mei et al., 2022). In silicate-bearing ores an additional dehydroxylation contribution from clay-like phases falls in the same window, with reported activation energies of 35–60 kcal mol^{-1} for kaolinite-type structures (Polcowñuk Iriarte et al., 2025). As a consequence, the integrated mass loss between 700 and 850 °C cannot be assigned to calcite by inspection of the TG curve alone, and the carbonate signal must be cross-checked against an independent measurement.

The magnitude of the competing thermal signals must also be considered if calcite is to be identified by both mass loss and heat flow. Calorimetric measurements have established formation enthalpies for the Mn-oxide end-members and constrain the heat budget of each redox step (Birkner & Navrotsky, 2017), while crystallographic compilations describe the structural relationships between the phases that coexist during reduction. Simultaneous TGA/DSC/XRD analysis of mechanically activated Mn_3O_4 has resolved its oxidation behaviour as a stepwise transformation through Mn_2O_3, with mass changes of several wt.% in the 400–800 °C interval (Berbenni & Marini, 2003). Pyrometallurgical surveys of Mn-ore feedstock report cumulative pre-smelting mass losses that combine calcite decarbonation with Mn-oxide reduction and water release

(Gordon et al., 2018), confirming that the bulk thermal record of a Mn ore is intrinsically multi-source. These reference data fix the order of magnitude of the non-carbonate background against which any TGA-based calcite assignment in such a matrix must be performed.

Several analytical strategies are available to address this overlap. X-ray diffraction with Rietveld refinement is the most direct phase-sensitive route (Dos Santos et al., 2017), but its accuracy degrades when the sample contains a substantial X-ray amorphous fraction or when carbonate stoichiometry deviates from pure end-members (Akinbodunse et al., 2024; Gualtieri, 2000). Wet-chemical decarbonation under acid attack is destructive and slow. Coupled TG–MS resolves CO_2 evolution and reaches detection limits below 100 ppm of calcite (Bartels et al., 2024), at the cost of an instrumental complexity not always available in routine ore-control laboratories. Rock-Eval analysis offers comparable kinetic resolution and is widely used for sedimentary carbonates (Baudin et al., 2023). X-ray fluorescence delivers the bulk Ca content quickly and with low uncertainty (Chubarov et al., 2020; Pashkova et al., 2020), but, by itself, does not distinguish carbonate-bound from silicate-bound Ca, and remains sensitive to sample preparation effects in heterogeneous ore powders. None of these methods, taken alone, combines high throughput with an unambiguous Ca-phase assignment for Mn-rich ores.

In summary, none of the bulk methods reviewed above provides unambiguous calcite quantification in Mn-rich ores when used in isolation. The remainder of this work tests whether the combined use of TGA and XRF can fill this gap by treating the disagreement between two independent calcite estimates as a diagnostic of carbonate-bound calcium. The framework relies on standard error-propagation rules (Vyazovkin et al., 2011).

Materials and methods. Objects of study. Two manganese ores from the Atasu mineralogical province of Central Kazakhstan were selected as a contrasting pair. The first sample, taken as the positive control, was an oxide–carbonate ore from the Bogach deposit (Nurinsky district of the Karaganda region; coordinates 49°44′43.4″ N, 68°57′16.5″ E). The deposit is of metamorphosed sedimentary type. A previous Rietveld refinement of the as-received material returned a mineralogical assemblage dominated by cryptomelane and hollandite (about 70.6 wt.%) together with braunite (10.4 wt.%), calcite (8.4 wt.%), bixbyite (6.4 wt.%) and quartz (4.3 wt.%) (Safarov et al., 2021). The second sample, taken as the negative control, was a silicate-bearing braunite ore from the Zhaksy deposit (Zhaksy district of the Akmola region; coordinates 51°56′26.7″ N, 67°21′52.1″ E), in which braunite and quartz are the dominant phases and crystalline calcite is below the XRD detection limit (Safarov et al., 2021, 2025). Together the two samples span the principal range of Ca-phase configurations encountered in the Atasu province and offer the maximum methodological contrast at the minimum number of test specimens.

Sample preparation. Both ores were processed by an identical scheme. Lump material was crushed in a jaw crusher to a particle size below 5 mm and then milled in a Pulverisette-7 PL planetary mill (Fritsch, Germany) at 400 rpm for 4 h with hardened-steel grinding bodies. The milled powder was passed through a 75 μm sieve to obtain

the analytical fraction, after which it was dry-homogenised in a closed container for 30 min on a roller mixer to suppress segregation prior to the TGA, XRF and XRD measurements.

Thermogravimetric and differential scanning calorimetry analysis. Simultaneous thermogravimetric and differential scanning calorimetry measurements were carried out on a Labsys Evolution TG-DTA/DSC instrument (Setaram, France) using corundum (Al_2O_3) crucibles. Sample masses ranged from 10 to 20 mg. Each sample was heated from 30 to 1200 °C at a constant rate of 10 K/min under a flow of dry nitrogen of 30 mL/min. A baseline correction was applied by recording an empty-crucible run under identical conditions and subtracting it from the sample signal. Mass-loss intervals were defined by the inflection points of the dTG curve, and DSC integrals were obtained by linear-baseline integration in the Setaram Calisto software.

X-ray fluorescence spectroscopy. The bulk elemental composition was determined by wavelength-dispersive X-ray fluorescence spectroscopy on an S2 Puma benchtop spectrometer (Bruker, Germany) equipped with a silver anode operated in the range from 20 to 50 kV under vacuum. Pressed tablets were prepared by the sandwich technique: 5 g of homogenised ore powder were laid over a 9 g layer of boric acid serving as the backing, and the assembly was compacted at a load of 25 t for 30 s in a steel die. Quantitative calibration of the major-element channels relied on the factory parameter set of the instrument, and the reported wt.% values for Mn, Ca, Si, Fe and other elements were taken directly from the standard output of the Bruker Spectra.Elements software.

X-ray diffraction. The qualitative and quantitative mineralogical composition of the as-received ores was investigated by X-ray powder diffraction on a D6 Phaser benchtop diffractometer (Bruker, Germany) using copper Kα radiation (λ = 1.5406 Å). The X-ray tube was operated at 40 kV and 15 mA. Diffractograms were recorded in the 2θ range from 15 to 85° with a step size of 0.02° and a counting time of 0.8 s per step. The sample was rotated at 10 rpm throughout the measurement in order to suppress preferred-orientation effects. Phase identification and Rietveld refinement of the recorded patterns were performed in Profex v5.4.0 against structural models drawn from the Crystallography Open Database (revision 240108). XRD served as an external method for cross-checking the outcome of the TGA–XRF protocol rather than as the basis of the quantitative calculation in the present work.

Quantitative calculations. The TGA-based calcite estimate is obtained from the mass loss in the decarbonation window, equation (1):

$$w_{CaCO_3}^{TGA} = \frac{\Delta m_{decarb}}{M(CO_2) / M(CaCO_3)} = \frac{\Delta m_{decarb}}{0.4397}, \quad (1)$$

where Δm_{decarb} is the mass loss in the decarbonation stage (wt.%), $M(CO_2)$ = 44.009 g/mol, $M(CaCO_3)$ = 100.087 g/mol. The ratio 0.4397 is the mass fraction of CO_2 in calcite.

The XRF-based estimate follows from the Ca content and the $CaCO_3$/Ca mass ratio, equation (2):

$$w_{CaCO_3}^{XRF} = w_{Ca}^{XRF} \cdot \frac{M(CaCO_3)}{M(Ca)} = w_{Ca}^{XRF} \cdot 2.4973, \quad (2)$$

where w_{Ca}^{XRF} is the Ca mass fraction by XRF and $M(Ca)$ = 40.078 g/mol. The coefficient 2.4973 = 100.087 / 40.078.

The consistency between the two estimates was assessed through their relative discrepancy $\delta = (w_{TGA} - w_{XRF})/w_{TGA} \times 100\,\%$. The acceptance threshold ($|\delta| \lesssim 5$ %) was derived from standard error propagation of the input uncertainties at the working composition rather than postulated, and is specific to the present measurement regime (10 K/min, N_2); for other heating rates, atmospheres or Ca levels it is re-evaluated by the same procedure.

Results.

Bulk elemental composition

Major-element XRF data for the two ores are shown in Figure 1. Bogach contains Mn 60.77 wt.%, Ca 5.44 wt.%, Si 3.49 wt.% and Fe 0.89 wt.%. Zhaksy contains Mn 44.88 wt.%, Ca 0.76 wt.%, Si 20.85 wt.% and Fe 6.14 wt.%. The seven-fold contrast in Ca content (5.44 vs. 0.76 wt.%) and the six-fold contrast in Si (3.49 vs. 20.85 wt.%) define the two samples as a carbonate-bearing and a silicate-bearing end-member. Fe is enriched in Zhaksy by a factor of seven and indicates a larger Fe-silicate fraction.

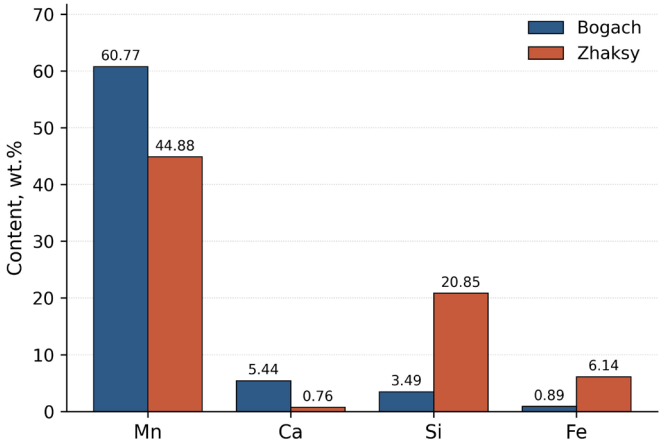

Figure 1 – Bulk elemental composition of the Bogach and Zhaksy manganese ores by XRF (wt.%; Mn, Ca, Si, Fe).

Thermal behaviour of the Bogach ore

Figure 2 shows the TG and dTG curves of Bogach recorded at 10 K/min under N_2. The total mass loss at 1200 °C is 27.44 wt.%. Mass release is distributed across several intervals. The largest single step lies in the 693–836 °C window. It produces a sharp dTG minimum at 714 °C with a rate of −1.21 %/min and accounts for 6.30 wt.% of the total mass loss. Smaller steps below 693 °C are attributed to adsorbed water release (30–200 °C), dehydroxylation (200–364 °C), the $MnO_2 \rightarrow Mn_2O_3$ transition (365–495 °C)

and cryptomelane–hollandite breakdown (557–693 °C). Above 911 °C the TG baseline drifts downward by an additional 6 wt.%, consistent with the $Mn_2O_3 \rightarrow Mn_3O_4$ step and partial sintering.

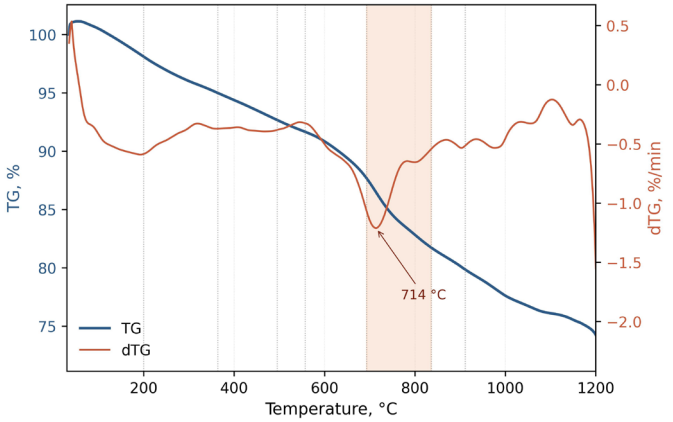

Figure 2 – TG and dTG curves of the Bogach ore (10 K/min, N_2, Al_2O_3 crucible). Decarbonation window 693–836 °C is shaded; dTG minimum at 714 °C is marked.

The DSC curve of Bogach (Figure 3) carries two endothermic features separated by a broad exothermic envelope. The low-temperature peak is centred at 215 °C with an integrated enthalpy of 96 J/g over the narrow window 38–272 °C. This window corresponds to desorption of physically adsorbed moisture and the loss of any weakly bound hydroxyl species from the ore surface. Compared with the Zhaksy counterpart (146 J/g over a wider 32–381 °C window), the Bogach low-T event is smaller in both enthalpy and temperature extent, in line with the lower silicate fraction (Si 3.49 wt.% against 20.85 wt.% in Zhaksy) and the consequently smaller contribution from silicate dehydroxylation.

Between 300 and 600 °C the DSC signal rises above the baseline into a broad exothermic envelope. The envelope is the superposition of the oxidative $MnO_2 \rightarrow Mn_2O_3$ transition in the cryptomelane and hollandite tunnel phases, which proceeds exothermically under the carrier gas atmosphere used here, with residual dehydroxylation of OH-bearing phases (Berbenni & Marini, 2003; Song et al., 2023). The exothermic maximum near 440 °C brackets the dTG stage attributed to the $MnO_2 \rightarrow Mn_2O_3$ transition

The high-temperature endothermic event is centred at 721 °C with an integrated enthalpy of 3536 J/g over 498–1213 °C, with the minimum at 723 °C and −27.9 mW. The temperature, the magnitude of the integrated heat and the temperature co-registration with the dTG minimum at 714 °C (offset +9 °C) jointly identify this event as the decarbonation of $CaCO_3$ (Rodriguez-Navarro et al., 2009) under the standard enthalpy of about 178 kJ mol^{-1} of calcite. Minor contributions from continuing Mn-oxide reduction above 700 °C and from the onset of sintering add a broad tail to the endotherm extending to 1213 °C, but they do not displace the minimum from the calcite decarbonation range.

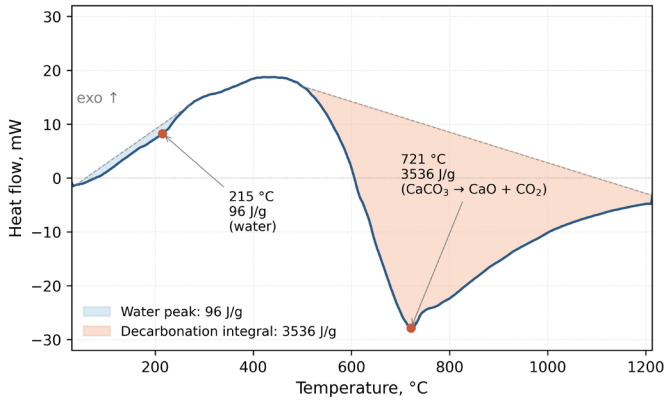

Figure 3 – DSC curve of the Bogach ore.
Low-temperature shoulder (215 °C, 96 J/g) and high-temperature endotherm (721 °C, 3536 J/g over 569–1213 °C) are labelled.

Thermal behaviour of the Zhaksy ore

The TG and dTG curves of Zhaksy are shown in Figure 4. The total mass loss at 1200 °C is 12.33 wt.%, less than half of the Bogach value. The dTG profile contains no sharp step comparable to the 714 °C feature of Bogach. Within the 723–922 °C window the only minimum is broad and shallow at −0.35 %/min at 806 °C, and the integrated mass loss in this window is 2.83 wt.%. The low-temperature dehydration stage below 400 °C is pronounced, in agreement with the higher clay and Fe-silicate content indicated by XRF.

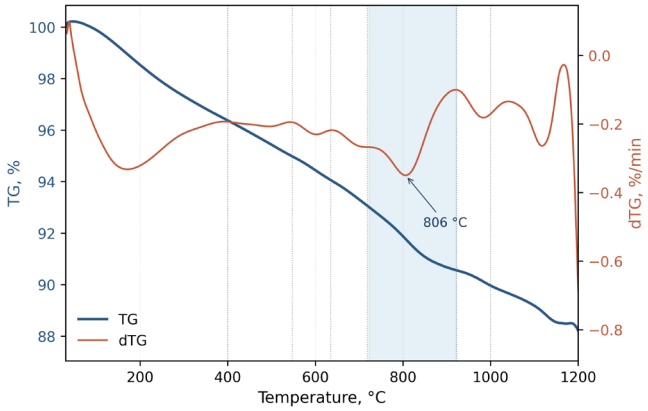

Figure 4 – TG and dTG curves of the Zhaksy ore (10 K/min, N_2).
The high-temperature window 723–922 °C is shaded in blue; the broad dTG minimum at 806 °C is marked.

The Zhaksy DSC curve (Figure 5) displays two endothermic events. The low-temperature peak is centred at 139 °C with an integrated enthalpy of 146 J/g over the window 32–381 °C. This window spans two overlapping mass-loss processes reported

by the TG curve below 400 °C – desorption of loosely bound moisture in the 30–150 °C range and subsequent dehydroxylation of OH-bearing silicate and Fe-oxyhydroxide phases between 150 and 381 °C. The integrated enthalpy of 146 J/g is consistent with the combined heat of evaporation of adsorbed water and the dehydroxylation of clay-like silicates (Polcowñuk Iriarte et al., 2025); the high silicate fraction of the Zhaksy ore (Si 20.85 wt.%, Fe 6.14 wt.%) explains the pronounced low-T event relative to the Bogach equivalent.

The high-temperature endotherm peaks at 729 °C with 537 J/g integrated over 467–1212 °C. The window covers a superposition of non-carbonate transformations. In the lower part of the window (467–700 °C) the Mn-oxide reduction chain $MnO_2 \rightarrow Mn_2O_3 \rightarrow Mn_3O_4$ releases lattice oxygen with an accompanying endothermic signal (Song et al., 2023), while residual dehydroxylation of silicates continues into the same interval. The deep minimum at 729 °C and the upper part of the window (700–1000 °C) reflect the onset of partial $Mn^{3+} \rightarrow Mn^{2+}$ reduction in the braunite structure – a mechanism analogous to the CLOU-type oxygen release documented for other Mn(III)-bearing phases (Mei et al., 2022) and consistent with the thermodynamics of Mn-oxide reduction established by calorimetric measurements on Mn-oxide end-members (Birkner & Navrotsky, 2017) – together with the onset of silicate recrystallisation in the silica-rich matrix. Relative to Bogach, the Zhaksy high-temperature enthalpy is 6.6 times smaller, while the dTG mass-loss ratio between the two ores in the same window is 2.2; the mismatch between the two ratios is the first indication that the Zhaksy signal is not dominated by a single decarbonation event. A broad exothermic envelope near 440 °C superimposed on the descending baseline indicates Mn-oxide redox activity accompanying the transitions above.

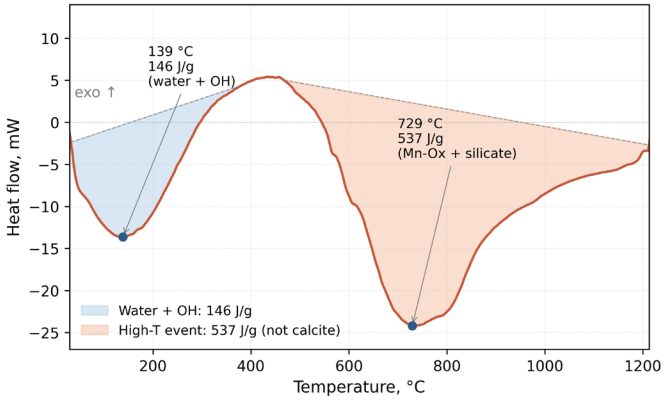

Figure 5 – DSC curve of the Zhaksy ore.
Low-temperature peak (139 °C, 146 J/g) and high-temperature endotherm (729 °C, 537 J/g over 467–1212 °C) are labelled.

Co-registration of dTG and DSC

The co-registration test places the two instrumental channels on a common temperature axis and measures the offset between their minima inside the putative

carbonate window. At 10 K/min a single decarbonation event produces a dTG minimum that leads the DSC minimum by a small kinetic lag.

For Bogach (Figure 6) the dTG minimum lies at 714 °C and the DSC minimum at 723 °C. The offset is +9 °C. This value is within the range expected for a common mass-release and heat-uptake process.

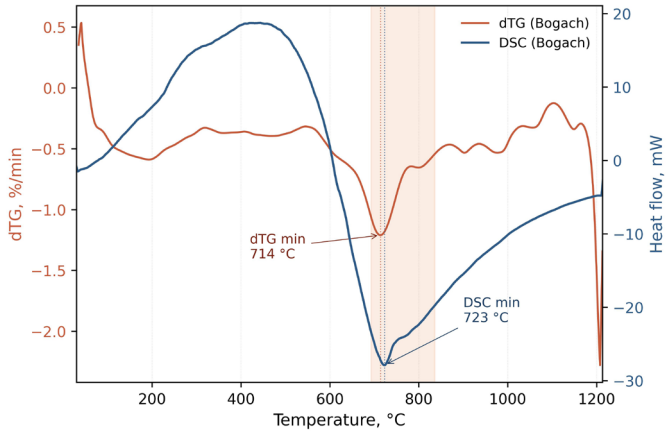

Figure 6 – Co-registration of dTG (Bogach, red) and DSC (Bogach, blue) on a common temperature axis.
The dTG minimum (714 °C) and DSC minimum (723 °C) fall within +9 °C of each other.

For Zhaksy (Figure 7) the broad dTG minimum lies at 806 °C and the DSC minimum at 729 °C. The offset is +77 °C, almost an order of magnitude larger than for Bogach. The two channels peak in different parts of the 700–900 °C interval.

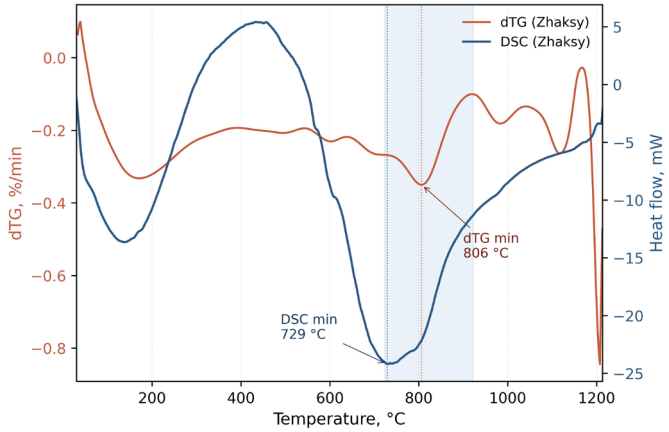

Figure 7 – Co-registration of dTG (Zhaksy, red) and DSC (Zhaksy, blue).
The dTG minimum (806 °C) and DSC minimum (729 °C) are separated by +77 °C, far above the kinetic-lag range expected for a common reaction.

Quantitative calcite estimates and the TGA–XRF cross-check

Equations (1) and (2) were applied to the decarbonation windows identified above. The stoichiometric constants used were $k_{TGA} = M(CO_2)/M(CaCO_3) = 0.4397$ and $k_{XRF} = M(CaCO_3)/M(Ca) = 2.4973$. Input values and outputs are listed in Table 1.

Table 1 – Calcite content derived from TGA (equation 1) and XRF (equation 2) and the relative discrepancy $\delta = (w_{TGA} - w_{XRF})/w_{TGA} \times 100\ \%$.

Sample	Δm_{decarb}, wt.%	w_{TGA}, wt.%	w_{Ca} (XRF), wt.%	w_{XRF}, wt.%	δ, %
Bogach	6.30	14.33	5.44	13.58	+5.2
Zhaksy	2.83	6.44	0.76	1.90	+70.5

Bogach sits at the +5.2 % boundary of the consistency band. Zhaksy exceeds the band by a factor of fourteen. Figure 8 maps both samples on the w_{TGA} vs. w_{XRF} diagnostic plane. Bogach falls on the upper edge of the ± 5 % envelope around the 1:1 line. Zhaksy lies far above the 1:1 line, in the region where w_{TGA} overestimates w_{XRF}.

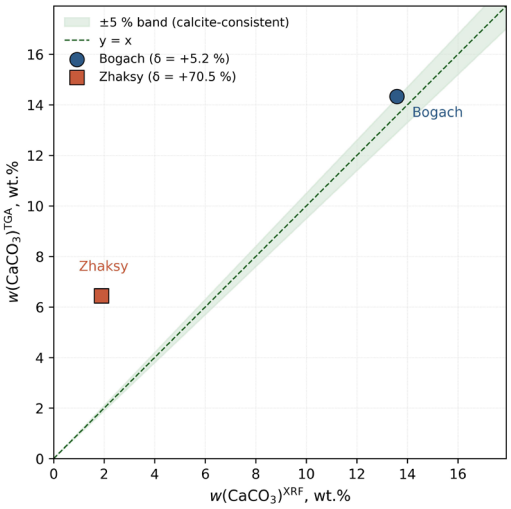

Figure 8 – Diagnostic diagram for the TGA–XRF cross-check.
Dashed line is the 1:1 reference; grey band is the ± 5 % consistency envelope. Bogach sits at the upper edge of the envelope; Zhaksy lies far above the 1:1 line.

Discussion.

The TGA–XRF cross-check as a diagnostic test

The decision rule rests on a simple mass balance. If all Ca measured by XRF is contained in calcite, equation (2) is exact. If the decarbonation window in the TGA is correctly identified, equation (1) is exact. Under these two assumptions the two estimates must coincide within the combined measurement uncertainty. Agreement between the two bulk estimates establishes the internal consistency of the carbonate hypothesis, not the absolute accuracy of the calcite content; both estimates are bulk-averaged upper bounds and are reconciled with the phase-resolved value in the XRD comparison below.

Two random sources dominate the uncertainty budget. The TGA mass-loss reading in a well-defined decarbonation window has a 1σ uncertainty of about 0.3 wt.%, accumulated from baseline drift, window-edge selection (±5 °C in the inflection-point procedure used here) and within-sample inhomogeneity after 4 h of planetary milling (Vyazovkin et al., 2011). The XRF Ca content in a sandwich-pressed pellet has a 1σ uncertainty of about 0.1 wt.% absolute at the 5 wt.% level, set by the calibration residuals and matrix correction of the factory parameter set on the S2 Puma (Chubarov et al., 2020). The stoichiometric constants $k_{TGA} = 0.4397$ and $k_{XRF} = 2.4973$ are exact and contribute no uncertainty.

Propagating these inputs through equations (1) and (2) gives the standard deviations of the two calcite estimates:

$$\sigma(w_{TGA}) = \frac{\sigma(\Delta m)}{k_{TGA}} = 0.68\ \text{wt.\%}, \tag{3}$$

$$\sigma(w_{XRF}) = \sigma(w_{Ca}) \cdot k_{XRF} = 0.25\ \text{wt.\%}. \tag{4}$$

The relative discrepancy between the two estimates is defined as

$$\delta = \frac{w_{TGA} - w_{XRF}}{w_{TGA}} \times 100\ \%, \tag{5}$$

with partial derivatives

$$\frac{\partial \delta}{\partial w_{TGA}} = \frac{w_{XRF}}{w_{TGA}^2} \times 100\ \%, \qquad \frac{\partial \delta}{\partial w_{XRF}} = -\frac{1}{w_{TGA}} \times 100\ \%. \tag{6}$$

Under the assumption of independent errors, σ(δ) follows from the standard quadrature rule:

$$\sigma(\delta) = \sqrt{\left(\frac{\partial \delta}{\partial w_{TGA}}\,\sigma(w_{TGA})\right)^2 + \left(\frac{\partial \delta}{\partial w_{XRF}}\,\sigma(w_{XRF})\right)^2}. \tag{7}$$

At the Bogach working point ($w_{TGA} = 14.33$ wt.%, $w_{XRF} = 13.58$ wt.%) the partial derivatives evaluate to 0.0661 and -0.0698 per wt.%, which, substituted into equation (7), give $\sigma(\delta) = \sqrt{(0.0661 \times 0.68)^2 + (0.0698 \times 0.25)^2} \times 100\ \% \approx 4.8\ \%$. The 1σ uncertainty band on δ is therefore close to 5 %. Inputs and propagated outputs are summarised in Table 2.

Table 2 – Uncertainty budget for the TGA–XRF cross-check at the Bogach point. Stoichiometric factors $k_{TGA} = M(CO_2)/M(CaCO_3) = 0.4397$ and $k_{XRF} = M(CaCO_3)/M(Ca) = 2.4973$ are treated as exact.

Source	Symbol	1σ value
TGA mass-loss reading	σ(Δ m)	0.30 wt.%
XRF Ca content	$\sigma(w_{Ca})$	0.10 wt.%
Propagated TGA calcite	$\sigma(w_{TGA})$	0.68 wt.%
Propagated XRF calcite	$\sigma(w_{XRF})$	0.25 wt.%
Propagated relative discrepancy at the Bogach point	σ(δ)	4.8 %

The acceptance threshold is therefore the 1σ band derived from propagated measurement errors rather than a postulated value. Because the propagated value σ(δ) = 4.8 % rounds to 5 %, the band is properly read as an approximate 1σ limit ($|\delta| \lesssim 5$ %) and not as a sharp cut-off, and a measured δ is judged against it within its propagated 1σ uncertainty (±4.8 % at the Bogach point). A sample whose discrepancy does not significantly exceed this band – that is, whose δ remains statistically indistinguishable from zero at the 1σ level – is consistent with a single-phase calcite assignment within measurement error. A sample whose discrepancy exceeds the band by several standard deviations requires an alternative explanation of the mass loss in the high-temperature window. The use of disagreement between two bulk methods as a phase-speciation diagnostic follows the broader pattern in carbonate analytics, in which TG–MS, Rock-Eval and XRD have been combined to validate one another for sedimentary materials (Bartels et al., 2024; Baudin et al., 2023); the present formulation transposes that logic to a Mn-rich matrix in which all three single-method routes carry phase ambiguity.

Calcite assignment in the Bogach ore

For Bogach the two estimates agree to δ = +5.2 %, carrying a propagated 1σ uncertainty of ±4.8 % (Table 2). The point estimate exceeds the nominal 5 % limit by only 0.4 percentage points — an order of magnitude smaller than its own uncertainty — and the discrepancy interval (+5.2 ± 4.8 %) overlaps both zero and the threshold. Bogach therefore lies on the 1σ boundary of the consistency band and is statistically indistinguishable from it; this is the sense in which the sample is classified as consistent, rather than as falling below an exactly defined 5.000 % line. Three further observations support the calcite assignment for the 693–836 °C step. First, the dTG peak at 714 °C lies within the accepted temperature range for calcite decarbonation at 10 K/min in N_2 (700–850 °C).

Second, the DSC endotherm peaks at 721 °C, within +9 °C of the dTG minimum. The kinetic lag between mass release and heat uptake has the expected sign and magnitude for a single decarbonation event.

Third, the XRF-based estimate (13.58 wt.%) sits below the TGA value (14.33 wt.%). The sign of the discrepancy is the one expected when a small fraction of the 693–836 °C mass loss originates from residual Mn-oxide or hydroxyl contributions rather than from decarbonation. The TGA value is therefore an upper bound and the XRF value a lower bound on the true calcite content in Bogach.

Enthalpy budget rules out decarbonation in Zhaksy

The Zhaksy cross-check fails by a wide margin (δ = +70.5 %). The independent enthalpy budget confirms that failure. The standard enthalpy of $CaCO_3$ decarbonation is about 178 kJ mol^{-1} (Rodriguez-Navarro et al., 2009), or 1778 J per gram of calcite.

The XRF-based upper bound on the calcite content in Zhaksy is 1.90 wt.%. Complete decarbonation of this amount would release 1.90 × 17.78 = 33.8 J per gram of ore. The DSC integral in the 467–1212 °C window is 537 J/g, sixteen times higher than any plausible calcite contribution.

The excess enthalpy and the mass loss itself originate from non-carbonate chemistry. X-ray diffraction of the as-received Zhaksy ore shows braunite (nominal Mn_7SiO_{12}, containing both Mn^{3+} and Mn^{2+}) as the dominant manganese phase, with no calcite and no hausmannite detected. Under N_2 above 700 °C two processes contribute to the 723–922 °C window. The lower part of the window (≈700–800 °C) is dominated by dehydroxylation of OH-bearing silicates. The upper part (≈800–900 °C) reflects the onset of partial $Mn^{3+} \rightarrow Mn^{2+}$ reduction in the braunite structure with limited oxygen release. The full braunite → hausmannite + silicate transformation proceeds above 1000 °C, outside the integration window used here, and has been observed independently in SQUID magnetometry of heated Zhaksy material. The 2.83 wt.% Δm therefore represents a precursor stage of these non-carbonate reactions, not calcite decarbonation.

Co-registration of the two channels as an independent check

The mass-loss and heat-flow channels of a simultaneous TGA–DSC record the same event at slightly different times. At 10 K/min the kinetic lag rarely exceeds 10–15 °C for a single-step reaction. The +9 °C offset measured for Bogach (Figure 6) lies inside this range.

The +77 °C offset measured for Zhaksy (Figure 7) cannot be rationalised as a kinetic lag. The two channels must therefore respond to different underlying reactions. The dTG minimum at 806 °C tracks the onset of $Mn^{3+} \rightarrow Mn^{2+}$ reduction in braunite with slow oxygen release. The DSC minimum at 729 °C tracks silicate dehydroxylation, which releases less mass but more heat per unit mass and therefore dominates the DSC signal at a lower temperature than the dTG signal.

Co-registration requires no stoichiometric assumption. It adds a second independent criterion to the TGA–XRF cross-check. It is particularly useful when the XRF Ca value is low (below 1 wt.%) and equation (2) becomes numerically noisy.

Comparison with XRD Rietveld phase analysis

The TGA–XRF cross-check returned $w(CaCO_3)$ ≈ 14 wt.% for the Bogach ore, whereas an independent XRD Rietveld refinement of the same material yields a calcite phase fraction of 8.4 wt.% (Safarov et al., 2021). The two values differ by 5–6 wt.% absolute, well beyond the combined TGA + XRF uncertainty established in the uncertainty budget above. The discrepancy is informative about the limitations of each method and is examined here.

Three contributions plausibly account for the gap. First, the Rietveld refinement was performed without an internal standard, so the reported phase fractions are normalised on a 100 % crystalline basis. If the sample contains a non-negligible X-ray

amorphous component, this normalisation acts in opposite ways for different phases. With cryptomelane and hollandite as the dominant Mn-oxide carriers in Bogach, both characterised by large unit cells with intrinsic tunnel disorder and moderate peak broadening (Birkner & Navrotsky, 2017), part of the diffracted intensity from these phases distributes into the amorphous halo and escapes the structural model. A formal correction with corundum as internal standard is the established remedy (Gualtieri, 2000) but was not applied in the original refinement. Akinbodunse et al. (2024) report absolute errors within ±3 wt.% (95 % confidence interval) for internal-XRD-amorphous quantification and relative errors below 10 % once the amorphous fraction exceeds 10 wt.%, magnitudes commensurate with the gap observed here when the amorphous contribution is not explicitly refined.

Second, the calcite signal in a multiphase Mn-rich matrix is particularly vulnerable to peak overlap. The strongest calcite reflection at $2\theta \approx 29.4°$ ($d \approx 3.04$ Å, hkl 104) sits close to high-intensity reflections of cryptomelane and braunite at 28.7° and 32.9°, which broaden under tunnel disorder and Fe substitution, respectively. Fitting the 28–34° region without a fixed calcite occupancy can therefore redistribute intensity from calcite to the surrounding Mn phases. Non-stoichiometric carbonates (Mn- or Fe-substituted calcite) shift the reflections by up to 0.1° 2θ and broaden them, further depressing the apparent calcite fraction unless the substitution is refined explicitly (Dos Santos et al., 2017).

Third, the TGA and XRF estimates retain their own sources of bias. As noted in the calcite-assignment analysis above, the TGA window 693–836 °C may receive a residual contribution of 1–2 wt.% from continued breakdown of the cryptomelane/hollandite framework above 700 °C (Song et al., 2023), which inflates the apparent calcite mass loss. The XRF estimate assumes that all bulk Ca resides in calcite; even a small Ca-silicate fraction at the level of 0.5–1 wt.% Ca would shift $w(CaCO_3)^{XRF}$ down by 1.2–2.5 wt.%. Taken together, plausible adjustments push the TGA value down by 2–3 wt.%, the XRF value down by 1–2 wt.%, and, after correction for the amorphous fraction, the Rietveld value up by 2–4 wt.%. The three estimates then converge to a common range of 10–12 wt.% within their respective uncertainties.

The wider methodological implication is that the TGA–XRF cross-check and the Rietveld refinement carry complementary biases. The bulk methods are insensitive to crystallinity but vulnerable to overlap with non-carbonate mass losses and to Ca redistribution into other phases. The Rietveld refinement is phase-resolved but biased toward crystalline contributions and sensitive to peak-overlap effects in Mn-rich matrices. The TGA–XRF protocol therefore should be read as a screen for whole-sample carbonate balance rather than as a substitute for properly standardised Rietveld refinement when phase-resolved quantification is required.

Assumptions, limitations and scope

Two features of the present validation set its limits. The protocol was tested on a single measurement of one positive and one negative control, without replicate runs. The uncertainty budget in Table 2 is obtained analytically, by propagating literature and instrument-specification input uncertainties through equations (3)–(7), and not from

experimental repeatability; the propagated value $\sigma(\delta) = 4.8$ % is therefore a theoretical 1σ estimate that awaits confirmation on replicate measurements and on a larger, compositionally diverse sample set. In addition, the numerical values used throughout — the 700–850 °C decarbonation window, the $|\delta| \lesssim 5$ % acceptance threshold, the +10–15 °C dTG–DSC kinetic-lag range and the 178 kJ mol^{-1} decarbonation enthalpy – are tied to the specific measurement regime (10 K min^{-1} under flowing N_2) and, for the threshold, to the working composition of the Bogach point (≈14 wt.% $CaCO_3$). They are not universal constants of the method: a different heating rate, atmosphere or Ca level shifts both the decarbonation window and the propagated threshold, each of which must then be re-derived by the procedure of equations (3)–(7).

The protocol assumes that calcite is the only Ca-bearing phase above the XRF detection limit and that no other carbonate contributes significantly to the 700–850 °C window. Both assumptions must be checked sample-by-sample. In the Mn ores of Central Kazakhstan the main alternative Ca carriers are dolomite and manganocalcite. Dolomite would split the decarbonation into two dTG peaks near 750 and 850 °C. Manganocalcite would shift the onset to 650–700 °C and would also appear in XRD as a Mn carbonate. Neither feature is present in the Bogach data.

For ores with mixed carbonate mineralogy the protocol still returns a binary pass/fail verdict. A failed cross-check does not identify the interfering phase, only that calcite is not the dominant Ca carrier. In the present study the independent XRD patterns confirm both branches of the test directly: calcite is identified in Bogach, whereas Zhaksy shows braunite as the dominant Mn phase with no calcite above the XRD detection limit. XRD therefore serves here as an independent confirmation of the cross-check outcome rather than as a missing next step. Full quantitative phase attribution, including Rietveld refinement of all Mn-bearing phases and complete assignment of the individual dTG and DSC stages, lies outside the scope of the present methodological paper and is the subject of a companion study. Within its intended scope the TGA–XRF cross-check combined with dTG/DSC co-registration provides a rapid pre-screen (about 3 h per sample including sample preparation) that flags whether a full Rietveld refinement is required.

Conclusion. The present study examined a dual-method screening protocol that combines TGA–DSC and XRF measurements for the quantification of calcite in manganese-rich ores, on a paired sample set drawn from the Atasu province of Central Kazakhstan – the carbonate-bearing Bogach ore as a positive control and the silicate-bearing Zhaksy ore as a negative control. The principal results obtained in the course of the study are as follows.

1. A dual-method protocol for quantitative calcite assessment in carbonate-type manganese ores has been developed and verified, based on independent calculations of $\mathbf{w(CaCO_3)}$ from TGA-DSC and XRF.

2. For the Bogach ore the two estimates are $\mathbf{w(CaCO_3)}$ = 14.33 wt.% (TGA) and 13.58 wt.% (XRF); the relative discrepancy is δ = +5.2 %, which coincides with the propagated 1σ limit ($\sigma(\delta) = 4.8$ %) and is statistically indistinguishable from it.

3. The threshold $|\delta| \lesssim 5$ % is justified by error propagation and proposed as a

consistency criterion between the two methods and, simultaneously, as an indicator that no significant non-carbonate Ca-bearing phases are present.

4. The negative control on the Zhaksy ore (δ = +70.5 ‰) confirms the specificity of the protocol and is supported by an independent enthalpy balance: the measured DSC integral of 537 J/g is sixteen times higher than the maximum calcite contribution permitted by the XRF Ca value.

5. Co-registration of the dTG and DSC channels adds an independent diagnostic criterion. The +9 °C offset for Bogach and the +77 °C offset for Zhaksy distinguish a single decarbonation event from the superposition of Mn-oxide redox chemistry and silicate transformations.

6. Comparison with phase-resolved XRD Rietveld refinement shows that the bulk TGA–XRF protocol and the diffraction-based method carry complementary biases. The protocol is intended as a screen for whole-sample carbonate balance rather than as a substitute for an internally standardised Rietveld refinement when full phase-resolved quantification is required.

The work was directed at deriving an applicable analytical decision rule for Ca-phase speciation in Mn-rich matrices that does not rely on slow phase-resolved measurements. The results may find application in routine ore-control laboratories at the beneficiation stage of Mn feedstock processing for ferroalloy production and for Mn_3O_4 pigment manufacture, in the preliminary triage of unfamiliar Mn-ore samples prior to full Rietveld refinement, and as an input to energy balance calculations for the smelting stage where the calcite mass fraction directly governs the projected CaO yield and the corresponding CO_2 release.

References

Akinbodunse S.J., Ufer K., Dohrmann R., & Mikutta C. (2024) Evaluation of the Rietveld method for determining content and chemical composition of inorganic X-ray amorphous materials in soils. *American Mineralogist*, *109*(12). — P. 2037–2051. https://doi.org/10.2138/am-2023-9240 (in Eng.).

Bartels M.F., Miller Q.R.S., Cao R., Lahiri N., Holliman J.E., Stanfield C.H., & Schaef H.T. (2024) Parts-Per-Million Carbonate Mineral Quantification with Thermogravimetric Analysis–Mass Spectrometry. *Analytical Chemistry*, *96*(11). — P. 4385–4393. https://doi.org/10.1021/acs.analchem.3c03936 (in Eng.).

Baudin F., Bouton N., Wattripont A., & Carrier X. (2023) Carbonates thermal decomposition kinetics and their implications in using Rock-Eval® analysis for carbonates identification and quantification. *Science and Technology for Energy Transition*, *78*, 38. https://doi.org/10.2516/stet/2023038 (in Eng.).

Berbenni V., & Marini A. (2003) Oxidation behaviour of mechanically activated Mn3O4 by TGA/DSC/XRPD. *Materials Research Bulletin*, *38*(14). — P. 1859–1866. https://doi.org/10.1016/j.materresbull.2003.07.008 (in Eng.).

Birkner N., & Navrotsky A. (2017) Thermodynamics of manganese oxides: Sodium, potassium, and calcium birnessite and cryptomelane. *Proceedings of the National Academy of Sciences*, *114*(7). — P. 1162–1167. https://doi.org/10.1073/pnas.1620427114 (in Eng.).

Brusnitsyn A.I., Perova E.N., Vereshchagin O.S., Britvin S.N., Platonova N.V., & Shilovskhikh V.V. (2021) The Mineralogy of Iron and Manganese Ores of the Ushkatyn-III Deposit in Central Kazakhstan. *Geology of Ore Deposits*, *63*(8). — P. 772–792. https://doi.org/10.1134/S1075701521080031 (in Eng.).

Chubarov V.M., Amosova A.A., & Finkelshtein A.L. (2020) X-Ray Fluorescence Determination of Ore Elements in Ferromanganese Formations. *Inorganic Materials*, *56*(14). — P. 1423–1430. https://doi.org/10.1134/S0020168520140046 (in Eng.).

Dos Santos H., Neumann R., & Ávila C.A. (2017) Mineral Quantification with Simultaneous

Refinement of Ca-Mg Carbonates Non-Stoichiometry by X-ray Diffraction, Rietveld Method. *Minerals*, *7*(9), 164. https://doi.org/10.3390/min7090164 (in Eng.).

Gordon Y., Nell J., & Yaroshenko Y. (2018) Manganese Ore Thermal Treatment Prior to Smelting. *KnE Engineering*, *3*(5), 71. https://doi.org/10.18502/keg.v3i5.2656 (in Eng.).

Gualtieri A.F. (2000) Accuracy of XRPD QPA using the combined Rietveld–RIR method. *Journal of Applied Crystallography*, *33*(2). — P. 267–278. https://doi.org/10.1107/S002188989901643X (in Eng.).

Matsanga N., Tangstad M., Kalenga M.W., & Nheta W. (2025) Manganese Alloy Production─A Review of the SAF Process and Emerging Technologies. *ACS Omega*, *10*(39). — P.44840–44857. https://doi.org/10.1021/acsomega.5c05889 (in Eng.).

Mei D., Lyngfelt A., Leion H., Linderholm C., & Mattisson T. (2022) Oxygen Carrier and Alkali Interaction in Chemical Looping Combustion: Case Study Using a Braunite Mn Ore and Charcoal Impregnated with K2CO3 or Na2CO3. *Energy & Fuels*, *36*(17). — P. 9470–9484. https://doi.org/10.1021/acs.energyfuels.2c00553 (in Eng.).

Pashkova G.V., Chubarov V.M., Akhmetzhanov T.F., Zhilicheva A.N., Mukhamedova M.M., Finkelshtein A.L., & Belozerova, O. Yu. (2020). Total-reflection X-ray fluorescence spectrometry as a tool for the direct elemental analysis of ores: Application to iron, manganese, ferromanganese, nickel-copper sulfide ores and ferromanganese nodules. *Spectrochimica Acta Part B: Atomic Spectroscopy*, *168*, 105856. https://doi.org/10.1016/j.sab.2020.105856 (in Eng.).

Polcowñuk Iriarte I.A., Mocciaro A., Rendtorff N.M., & Richard D. (2025) Dehydroxylation of Kaolinite: Evaluation of Activation Energy by Thermogravimetric Analysis and Density Functional Theory Insights. *Minerals*, *15*(6), 607. https://doi.org/10.3390/min15060607 (in Eng.).

Rodriguez-Navarro C., Ruiz-Agudo E., Luque A., Rodriguez-Navarro A.B., & Ortega-Huertas M. (2009) Thermal decomposition of calcite: Mechanisms of formation and textural evolution of CaO nanocrystals. *American Mineralogist*, *94*(4). — P. 578–593. https://doi.org/10.2138/am.2009.3021 (in Eng.).

Safarov R.Z., Baikenov Y.A., Zhandildenova A.K., Kopishev E.E., Kamatov R.M., Kargin J.B., Sanchez Cornejo H., Barnes C.H.W., & De Los Santos Valladares L. (2025) Phase Transitions and Structural Evolution of Manganese Ores During High-Temperature Treatment. *Metals*, *15*(1), 89. https://doi.org/10.3390/met15010089 (in Eng.).

Safarov R.Z., Kargin J.B., Aibuldinov Y.K., Zhandildenova A.K., Makhmutov B.B., Sviderskiy A.K., & Vati N.I. (2021) Structure and content analysis of raw materials for production of trimanganese tetraoxide pigment. *Crystals*, *11*(12), 1460. https://doi.org/10.3390/cryst11121460 (in Eng.).

Song J., Liu M., Ma X., Tian Q., Feng J., Zhong X., & Duan F. (2023) Thermal decomposition behavior and computational analysis of alpha and beta manganese dioxide nanorods. *Journal of Alloys and Compounds*, *962*, 171208. https://doi.org/10.1016/j.jallcom.2023.171208 (in Eng.).

Vyazovkin S., Burnham A.K., Criado J.M., Pérez-Maqueda L.A., Popescu C., & Sbirrazzuoli N. (2011) ICTAC Kinetics Committee recommendations for performing kinetic computations on thermal analysis data. *Thermochimica Acta*, *520*(1–2). — P. 1–19. https://doi.org/10.1016/j.tca.2011.03.034 (in Eng.).

Zhuang D., Chen Z., & Sun B. (2025) Thermal Decomposition of Calcium Carbonate at Multiple Heating Rates in Different Atmospheres Using the Techniques of TG, DTG, and DSC. *Crystals*, *15*(2), 108. https://doi.org/10.3390/cryst15020108 (in Eng.).

Publication Ethics and Publication Malpractice
in the journals of the «Central Asian Academic Research Center» LLP (Almaty)

For information on Ethics in publishing and Ethical guidelines for journal publication see http://www.elsevier.com/publishingethics and http://www.elsevier.com/journal-authors/ethics.

Submission of an article to the National Academy of Sciences of the Republic of Kazakhstan implies that the described work has not been published previously (except in the form of an abstract or as part of a published lecture or academic thesis or as an electronic preprint, see http://www.elsevier.com/postingpolicy), that it is not under consideration for publication elsewhere, that its publication is approved by all authors and tacitly or explicitly by the responsible authorities where the work was carried out, and that, if accepted, it will not be published elsewhere in the same form, in English or in any other language, including electronically without the written consent of the copyright-holder. In particular, translations into English of papers already published in another language are not accepted.

No other forms of scientific misconduct are allowed, such as plagiarism, falsification, fraudulent data, incorrect interpretation of other works, incorrect citations, etc. The National Academy of Sciences of the Republic of Kazakhstan follows the Code of Conduct of the Committee on Publication Ethics (COPE), and follows the COPE Flowcharts for Resolving Cases of Suspected Misconduct (http://publicationethics.org/files/u2/New_Code.pdf). To verify originality, your article may be checked by the Cross Check originality detection service http://www.elsevier.com/editors/plagdetect.

The authors are obliged to participate in peer review process and be ready to provide corrections, clarifications, retractions and apologies when needed. All authors of a paper should have significantly contributed to the research.

The reviewers should provide objective judgments and should point out relevant published works which are not yet cited. Reviewed articles should be treated confidentially. The reviewers will be chosen in such a way that there is no conflict of interests with respect to the research, the authors and/or the research funders.

The editors have complete responsibility and authority to reject or accept a paper, and they will only accept a paper when reasonably certain. They will preserve anonymity of reviewers and promote publication of corrections, clarifications, retractions and apologies when needed. The acceptance of a paper automatically implies the copyright transfer to the National Academy of Sciences of the Republic of Kazakhstan.

The Editorial Board of the National Academy of Sciences of the Republic of Kazakhstan will monitor and safeguard publishing ethics.

Requirements for articles design for publication in the journal are available on the websites:
www:nauka-nanrk.kz
http://chemistry-technology.kz/index.php/en/arhiv
ISSN 2518-1491 (Online), ISSN 2224-5286 (Print)

Managing Editor: A.Shormakova
Editors: D.S. Alenov, T. Apendiev
Computer layout: G.D. Zhadyranova

Signed for print: June 30, 2026
Format: 70×90 1/16. 24.0 printed sheets. Order No. 2

«Central Asian Academic Research Center» LLP
Almaty, Shevchenko Street, 28